

Chapter 8

The general circulation of the atmosphere

In this chapter we return to our discussion of the large-scale circulation of the atmosphere and make use of the dynamical ideas developed in the previous two chapters to enquire into its cause. We begin by reviewing the demands on the atmospheric circulation imposed by global energy and angular momentum budgets as depicted in Fig.8.1. The atmosphere must transport energy from equator to pole to maintain the observed pole-equator temperature gradient. In addition, because there are westerly winds at the surface in middle latitudes and easterly winds in the tropics (see, e.g., Fig.7.28) angular momentum must be transported from the tropics to higher latitudes. We discuss how this transfer is achieved by the Hadley circulation in the tropics and weather systems in middle latitudes. We will discover that weather systems arise from a hydrodynamic instability of the thermal wind shear associated with the pole-equator temperature gradient. Produced through a mechanism known as baroclinic instability, the underlying dynamics are illustrated through laboratory experiment and discussed from the perspective of the available potential energy ‘stored’ by the horizontal temperature gradients.

8.1 Understanding the observed circulation

The simplest observed global characteristic of the atmosphere is that the tropics are much warmer than the poles. As discussed in Chapter 5, this

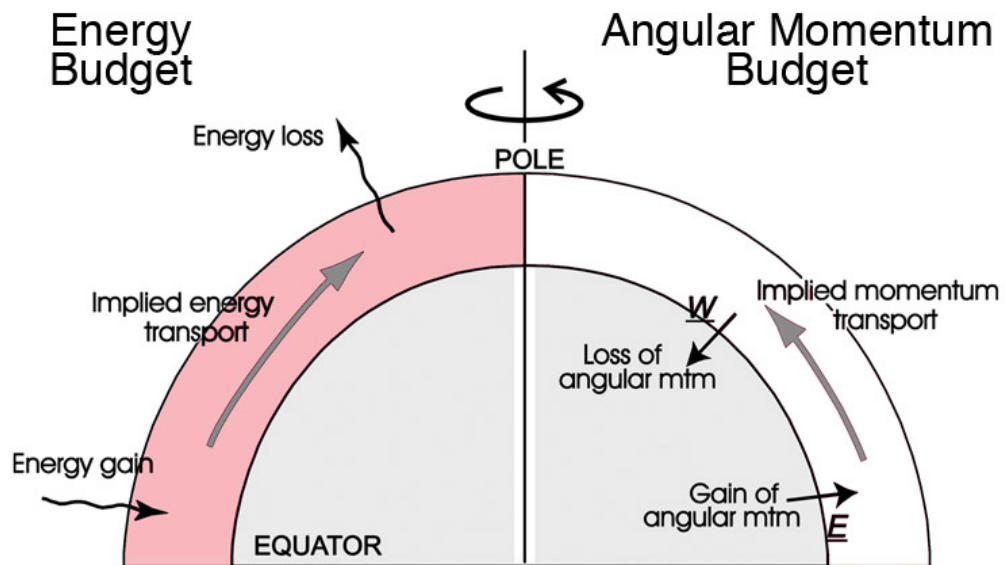


Figure 8.1: Latitudinal transport of (left) heat and (right) angular momentum implied by the observed state of the atmosphere. In the energy budget there is a net radiative gain in the tropics and a net loss at high latitudes; in order to balance the energy budget at each latitude, a poleward heat flux is implied. In the angular momentum budget the atmosphere gains angular momentum in low latitudes (where the surface winds are easterly) and loses it in middle latitudes (where the surface winds are westerly). A poleward atmospheric flux of angular momentum is thus implied.

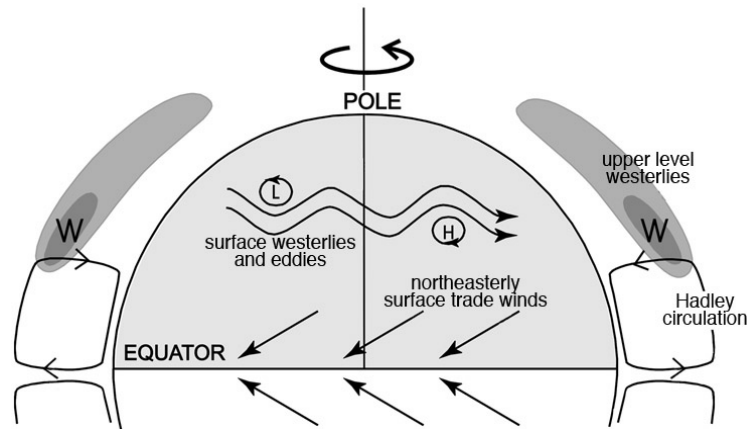


Figure 8.2: Schematic of the observed atmospheric general circulation for annual-averaged conditions. The upper level westerlies are shaded to reveal the core of the subtropical jet stream on the poleward flank of the Hadley circulation. The surface westerlies and surface trade winds are also marked, as are the highs and lows of middle latitudes. Only the northern hemisphere is shown. The vertical scale is greatly exaggerated.

is a straightforward consequence of the geometry of the earth: the annually averaged incoming solar radiation per unit area of the earth's surface is much greater at the equator than at the poles, a difference that is compounded by the fact that the polar regions are covered in ice and snow and therefore reflect much of the incoming radiation back to space. A little less obvious is the fact that the tropical regions actually receive more energy from the sun than they emit back to space, while the converse is true in high latitudes. Since both regions are, on an annual average, in equilibrium, there must be a process acting to transport excess energy from the tropics to make up the deficit in high latitudes, as depicted schematically in Fig.8.1(left).

The implied transport of some $6 \times 10^{15} \text{W}$ — see Fig.5.6 — must be effected by the atmospheric circulation, carrying warm air poleward and cold air equatorward. (In fact, the ocean circulation also contributes, as discussed in Chapter 11.) As a result, the tropics are cooler, and polar regions warmer, than they would be in the absence of such transport. Thus, in this as in other respects, the atmospheric general circulation plays a key role in climate.

What are the motions that deliver the required transport? The gross

features of the observed atmospheric circulation discussed in Chapter 5 are depicted in Fig.8.2. The zonal flow is strongly westerly aloft in middle latitudes, a fact that we can now, following Section 7.3, understand as a straightforward consequence of the decrease of temperature with latitude. Surface winds are constrained to be weak by the action of friction near the ground, and thermal wind balance, Eq.(7.24), implies that a poleward decrease of temperature is necessarily accompanied by increasing westerly winds with height. Taken together, these two facts require a zonal flow in middle latitudes that increases from near zero at the ground to strong westerlies at altitude, as schematized in Fig.7.19.

Although the near-surface winds are weak — a few m s^{-1} — they nevertheless exhibit a distinct spatial distribution, with the zonal component being easterly in the tropics and westerly in middle latitudes (Fig.7.28). In the presence of surface friction, the atmosphere must therefore be losing angular momentum to the ground in middle latitudes and gaining angular momentum in the tropics. As Fig.8.1(right) illustrates, the angular momentum balance of the atmosphere thus requires a transport of westerly angular momentum from low to middle latitudes in order to maintain equilibrium.

Even though the west-to-east circulation in the upper troposphere is the dominant component of the large-scale atmospheric flow, it cannot be responsible for the required poleward transports of heat and angular momentum, for which north-south flow is needed. As we saw in Chapter 5 (Fig.5.21) there is indeed a mean circulation in the meridional plane, which is dominated by the Hadley circulation of the tropical atmosphere with, on an annual average, mean upwelling near the equator, poleward flow aloft, subsidence in the subtropics and equatorward return flow near the surface. This circulation transports heat and angular momentum poleward, as required, within the tropics; however, the meridional circulation becomes much weaker in middle latitudes and so cannot produce much transport there. We saw in Section 5.4.1 that most of the north-south flow in the extratropical atmosphere takes the form of eddies, rather than a mean overturning as in the tropics. As we will see, it is these eddies that produce the poleward transports in the extra-tropics.

8.2 A mechanistic view of the circulation

To what extent can we explain the main features of the observed general circulation on the basis of the fluid dynamics of a simple representation of the atmosphere driven by latitudinal gradients in solar forcing? The emphasis here is on “simple”. In reality, the Earth’s surface is very inhomogeneous: there are large mountain ranges that disturb the flow and large contrasts (*e.g.*, in temperature and in surface roughness) between oceans and continents. In the interests of simplicity, however, we shall neglect such variations in surface conditions. We also neglect seasonal and diurnal¹ variations, and assume maximum solar input at the equator, even though the subsolar point (Fig.5.3) migrates between the two Tropics through the course of a year. Thus, we shall consider the response of an atmosphere on a longitudinally uniform, rotating, planet (that is otherwise like the Earth) to a latitudinal gradient of heating. We shall see that the gross features of the observed circulation can indeed be understood on this basis; later, in Section 8.5, the shortcomings introduced by this approach will be briefly discussed.

Thus, we ask how an axisymmetric atmosphere responds to an axisymmetric forcing, with stronger solar heating at the equator than at the poles. It seems reasonable to assume that the response (*i.e.*, the induced circulation) will be similarly axisymmetric. Indeed, this assumption turns out to give us a qualitatively reasonable description of the circulation in the tropics, but it will become evident that it fails in the extratropical atmosphere, where the symmetry is broken by hydrodynamical instability.

8.2.1 The tropical Hadley circulation

If the Earth were not rotating, the circulation driven by the pole-equator temperature difference would be straightforward, with warm air rising in low latitudes and cold air sinking at high latitudes as first suggested by Hadley and sketched in Fig.5.19. But, as seen in Figs.5.20 and 5.21, this is not quite what happens. We do indeed see a meridional circulation in the tropics, but the sinking motion is located in the subtropics around latitudes of

¹In reality, of course, there are strong instantaneous longitudinal variations in solar forcing between those regions around local noon and those in nighttime. However, except very near the surface, the thermal inertia of the atmosphere damps out these fluctuations and temperature varies little between day and night. Hence neglect of diurnal variations is in fact a reasonable approximation.

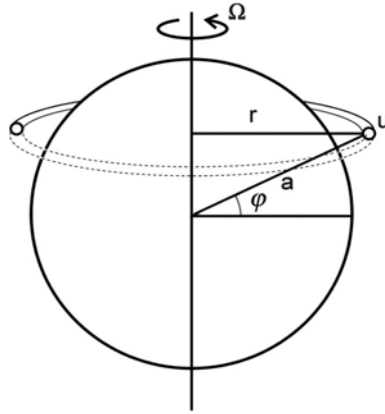


Figure 8.3: Schematic of a ring of air blowing west \longrightarrow east at speed u and latitude φ . The ring is assumed to be advected by the poleward flow of the Hadley circulation conserving angular momentum.

$\pm 30^\circ$. In fact, the following considerations tell us that one giant axisymmetric meridional cell extending from equator to pole is not possible on a rapidly rotating planet such as the Earth.

Consider a ring of air encircling the globe as shown in Fig.8.3, lying within, and being advected by, the upper level poleward flow of the Hadley circulation. Because this flow is, by assumption, axisymmetric and also because friction is negligible in this upper level flow, well above the near-surface boundary layer, absolute angular momentum will be conserved by the ring as it moves around. The absolute angular momentum per unit mass is (recall our discussion of angular momentum in the radial inflow experiment in Section 6.6.1)

$$A = \Omega r^2 + ur ,$$

the first term being the contribution from planetary rotation, and the second from the eastward wind u relative to the Earth, where r is the distance from the Earth's rotation axis. Since $r = a \cos \varphi$,

$$A = \Omega a^2 \cos^2 \varphi + ua \cos \varphi . \quad (8.1)$$

Now, suppose that $u = 0$ at the equator (Fig.5.20 shows that this is a reasonable assumption in the equatorial upper troposphere). Then the absolute angular momentum at the equator is simply $A_0 = \Omega a^2$. As the ring of air

moves poleward, it retains this value and so when it arrives at latitude φ , its absolute angular momentum is

$$A = \Omega a^2 \cos^2 \varphi + ua \cos \varphi = A_0 = \Omega a^2 .$$

Therefore the ring will acquire an eastward velocity

$$u(\varphi) = \frac{\Omega (a^2 - a^2 \cos^2 \varphi)}{a \cos \varphi} = \Omega a \frac{\sin^2 \varphi}{\cos \varphi} . \quad (8.2)$$

Note that this is directly analogous to Eq.(6.23) of our radial inflow experiment, when we realize that $r = a \cos \varphi$. Eq.(8.2) implies unrealistically large winds far from the equator: at latitudes of $(10^\circ, 20^\circ, 30^\circ)$, $u(\varphi) = (14, 58, 130) \text{ ms}^{-1}$, and of course the wind becomes infinite as $\varphi \rightarrow 90^\circ$. On the grounds of physical plausibility, it is clear that such an axisymmetric circulation cannot extend all the way to the pole in the way envisaged by Hadley (and sketched in Fig.5.19): it must terminate somewhere before it reaches the pole. Just how far the circulation extends depends (according to theory) on many factors².

Consider the upper branch of the circulation, as depicted in Fig.8.4. Near the equator, where f is small and the Coriolis effect is weak, angular momentum constraints are not so severe and the equatorial atmosphere acts as if the Earth were rotating slowly. As air moves away from the equator, however, the Coriolis parameter becomes increasingly large and, in the northern hemisphere, turns the wind to the right, resulting in a westerly component to the flow. At the poleward extent of the Hadley cell, then, we expect to find a strong westerly flow, as indeed we do — see Fig.5.20. This subtropical jet is driven in large part by the advection from the equator of large values of absolute angular momentum by the Hadley circulation, as is evident from Eq.(8.2) and depicted in Fig.8.4. Flow subsides on the subtropical edge of the Hadley cell, sinking into the subtropical highs (very evident in Fig.7.27), before returning to the equator at low levels. At these low levels, the Coriolis acceleration, again turning the equatorward flow to its right in the northern hemisphere, produces the “trade winds”, northeasterly in the northern hemisphere (southeasterly in the southern hemisphere) — see Fig.7.28. These winds are not nearly as strong as in the upper troposphere because they are moderated by friction acting on the near-surface

²For example, if the Earth were rotating less (or more) rapidly, and other things being equal, the Hadley circulation would extend further (or less far) poleward.

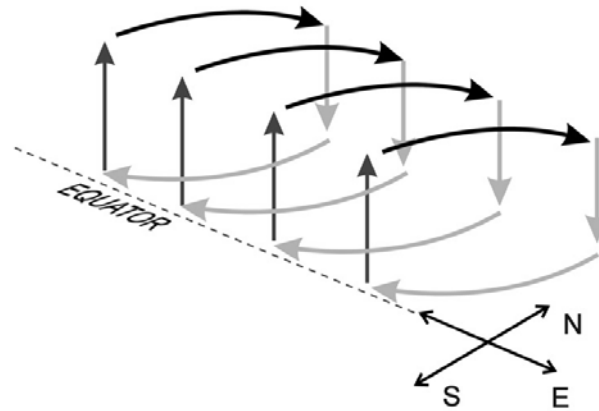


Figure 8.4: Schematic of the Hadley circulation (showing only the Northern Hemispheric part of the circulation; there is a mirror image circulation south of the equator). Upper level poleward flow induces westerlies; low level equatorward flow induces easterlies

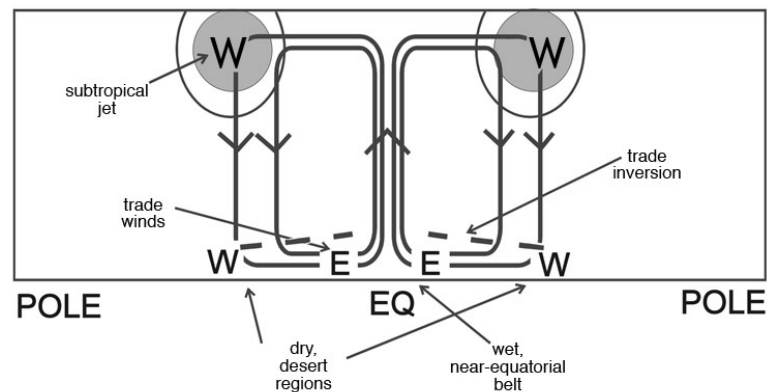


Figure 8.5: A schematic diagram of the Hadley circulation and its associated zonal flows and surface circulation.

flow. In fact, as discussed above, there must be low-level westerlies somewhere: in equilibrium, the net frictional drag (strictly, torque) on the entire atmosphere must be zero, or the total angular momentum of the atmosphere could not be steady. (There would be a compensating change in the angular momentum of the solid Earth, and the length of the day would drift³). So, as shown in Fig.8.5, the surface winds in our axisymmetric model would be westerly at the poleward edge of the circulation cell, and eastward near the equator. This is similar to the observed pattern (see Fig.7.28, middle panel), but not quite the same: in reality the surface westerlies maximize near 50°N, S, significantly poleward of the subtropical jet, a point to which we return in Section 8.4.2.

As sketched in Fig.8.5, the subtropical region of subsidence is warm (because of adiabatic compression) and dry (since the air aloft is much drier than surface air; the boundary formed between this subsiding air and the cooler, moister near-surface air is the “trade inversion” noted in Chapter 4 and within which the trade winds are located. Aloft, horizontal temperature gradients within the Hadley circulation are very weak — see Figs.5.7 and 5.8 — a consequence of very efficient meridional heat transport by the circulation.

Experiment on the Hadley circulation: GFD Lab VIII revisited

A number of aspects of the Hadley circulation are revealed in Expt VIII — whose experimental arrangement has already been described in Fig.7.12 in the context of the thermal wind equation. The apparatus is just a cylindrical tank containing plain water, at the center of which is a metal can filled with ice. The consequent temperature gradient (decreasing “poleward”) drives motions in the tank, the nature of which depends on the rotation rate of the apparatus. When slowly rotating, as in this experiment ($\Omega \lesssim 1$ rpm — yes, only 1 rotation of the table per minute: very slow!), we see the development of the thermal wind in the form of a strong “eastward” (*i.e.*, super-rotating) flow in the upper part of the fluid which can be revealed by paper dots floating on the surface and dye injected in to the fluid as seen in Fig.7.13.

³In fact the length of the day does vary, ever so slightly, due to angular momentum transfer between the atmosphere and underlying surface. For example on seasonal timescales there are changes in the length of the day of about a millisecond. The length of the day changes from day to day by about 0.1 ms! Moreover these changes can be attributed to exchanges of angular momentum between the earth and the atmosphere.

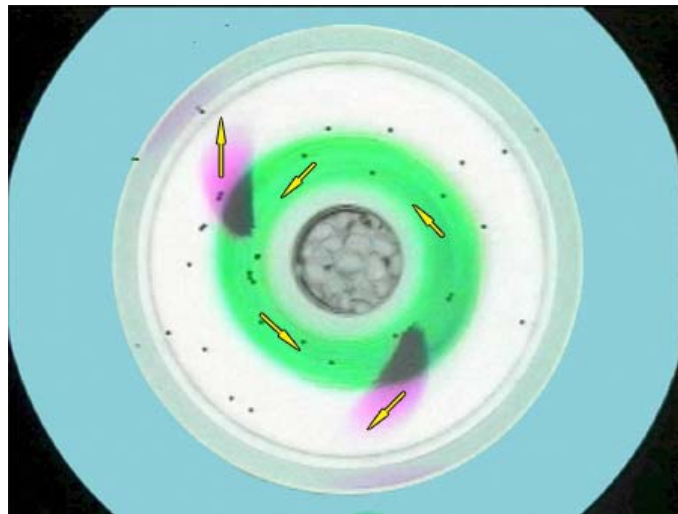


Figure 8.6: The Hadley regime studied in GFD Lab VIII, Section 7.3.1. Bottom flow is revealed by the two outward spiralling streaks showing anti-cyclonic (clockwise) flow sketched schematically in Fig.7.12(right); the black paper dots and collar of dye mark the upper level flow and circulate cyclonically (anticlockwise).

The azimuthal current observed in the experiment, which is formed in a manner analogous to that of the subtropical jet by the Hadley circulation discussed above, is maintained by angular momentum advection by the meridional circulation sketched in Fig.7.12(right). Water rises in the outer regions, moves inward in the upper layers, conserving angular momentum as it does so, thus generating strong “westerly” flow, and rubs against the cold inner wall, becoming cold and descending. Potassium permanganate crystals, dropped into the fluid (not too many!), settle on the bottom and give an indication of the flow in the bottom boundary layer. In Fig.8.6 we see flow moving radially outwards at the bottom and being deflected to the right, creating easterly flow in a direction opposite to that of the rotating table: note the two dark streamers moving outward and clockwise (opposite to the sense of rotation and the upper level flow). This bottom flow is directly analogous to the easterly and equatorward trade winds of the lower atmosphere sketched in Fig.8.4 and plotted from observations in Fig.7.28.

Quantitative study of the experiment (by tracking, for example, floating paper dots) shows that the upper level azimuthal flow does indeed conserve angular momentum, satisfying Eq.(6.23) quite accurately, just as in the radial inflow experiment. With $\Omega = 0.1 \text{ s}^{-1}$ (corresponding to a rotation rate of 0.95rpm — see Table 13.1, Appendix 13.4.1) Eq.(6.23) implies a hefty 10 cm s^{-1} if angular momentum were conserved by a particle moving from the outer radius $r_1 = 30 \text{ cm}$ to an inner radius of 30 cm. Note, however, that if Ω were set 10 times higher, to 10rpm, then angular momentum conservation would imply a speed of 1 m s^{-1} , a very swift current. We will see in the next section that such swift currents are not observed if we turn up the rotation rate of the table. Instead the azimuthal current breaks down into eddying motions, inducing azimuthal pressure gradients and breaking angular momentum conservation.

8.2.2 The extra-tropical circulation and GFD Lab XI: baroclinic instability

Although the simple Hadley cell model depicted in Fig.8.5 describes the tropical regions quite well, it predicts that little happens in middle and high latitudes. There, where the Coriolis parameter is much larger, the powerful constraints of rotation are dominant and meridional flow is impeded. We expect, however, (and have seen in Fig.5.8 and 7.20), that there are strong

gradients of temperature in middle latitudes, particularly in the vicinity of the subtropical jet. So, although there is little meridional circulation, there is a zonal flow in thermal wind balance with the temperature gradient: since T decreases poleward, Eq.(7.24) implies westerly winds increasing with height. This state of a zonal flow with no meridional motion is a perfectly valid equilibrium state: even though the existence of a horizontal temperature gradient implies horizontal pressure gradients (tilts of pressure surfaces), the associated force is entirely balanced by the Coriolis force acting on the thermal wind, as we discussed in Chapter 7.

Our deduction that the mean meridional circulation is weak outside the tropics is qualitatively in accord with observations (see Fig.5.21) but leaves us with two problems:

1. Poleward heat transport is required to balance the energy budget. In the tropics, the overturning Hadley circulation transports heat poleward, but no further than the subtropics. How is heat transported further poleward if there is no meridional circulation?
2. Everyday observation tells us that a picture of the midlatitude atmosphere as one with purely zonal winds is very wrong. If it were true, weather would be very predictable (and very dull).

Our axisymmetric model is, therefore, only partly correct. The prediction of purely zonal flow outside the tropics is quite wrong. As we have seen, the midlatitude atmosphere is full of *eddies*, which manifest themselves as traveling weather systems.⁴ Where do they come from? In fact, as we shall now discuss and demonstrate through a laboratory experiment, the extratropical atmosphere is hydrodynamically unstable, the flow spontaneously



⁴ Albert Defant (1884 – 1974) German Professor of Meteorology and Oceanography, who made important contributions to the theory of the general circulation of the atmosphere. He was the first to liken the meridional transfer of energy between the subtropics and pole to a turbulent exchange by large-scale eddies.

breaking down into eddies through a mechanism known as baroclinic instability⁵. These eddies readily generate meridional motion and, as we shall see, effect a meridional transport of heat.

Baroclinic instability

GFD Lab XI — baroclinic instability in a dishpan To introduce our discussion of the breakdown of the thermal wind through baroclinic instability we describe a laboratory experiment of the phenomenon. The apparatus, sketched in Fig.7.12, is identical to that of Lab VIII used to study the thermal wind and the Hadley circulation. In the former experiments the table was rotated very slowly, at a rate of $\Omega \lesssim 1$ rpm. This time, however, the table is rotated much more rapidly, at $\Omega \sim 10$ rpm, representing the considerably greater Coriolis parameter found in middle latitudes. At this higher rotation rate something remarkable happens. Rather than a steady axisymmetric flow, as in the Hadley regime shown in Fig.8.6, a strongly eddying flow is set up. The thermal wind remains, but breaks down through instability, as shown in Fig.8.7. We see the development of eddies which sweep (relatively) warm fluid from the periphery to the cold can in one sector of the tank (e.g. A in Fig.8.7) and, simultaneously, carry cold fluid from the can to the periphery at another (e.g. B in Fig.8.7). In this way a radially-inward heat transport is achieved, offsetting the cooling at the centre caused by the melting ice.

For the experiment shown we observe three complete wavelengths around the tank in Fig.8.7. By repeating the experiment but at different values of Ω , we observe that the scale of the eddies decreases and the flow becomes increasingly irregular as Ω is increased. These eddies are produced by the same mechanism at work in the creation of atmospheric weather systems shown in Fig.7.20 and discussed below.

Before going on we should emphasize that the flow in Fig.8.7 does not conserve angular momentum. Indeed, if it did, as estimated at the end of Section 8.2.1, we would observe very strong horizontal currents near the ice bucket, of order 1 m s^{-1} rather than a few cm s^{-1} as seen in the experiment. This, of course, is exactly what Eq.(8.2) is saying for the atmosphere: if rings of air conserved angular momentum as they move in axisymmetric motion

⁵In a ‘baroclinic’ fluid $\rho = \rho(p, T)$ and so there can be gradients of density (and therefore of temperature) along pressure surfaces. This should be contrasted to a ‘barotropic’ fluid ($\rho = \rho(p)$) in which no such gradients exist.



Figure 8.7: (Top) Baroclinic eddies in the 'eddy' regime viewed from the side. (Bottom) View from above. Eddies draw fluid from the periphery in toward the centre at point A and vice-versa at point B. The eddies are created by the instability of the thermal wind induced by the radial temperature gradient due to the presence of the ice bucket at the centre of the tank. The diameter of the ice bucket is 15 cm.

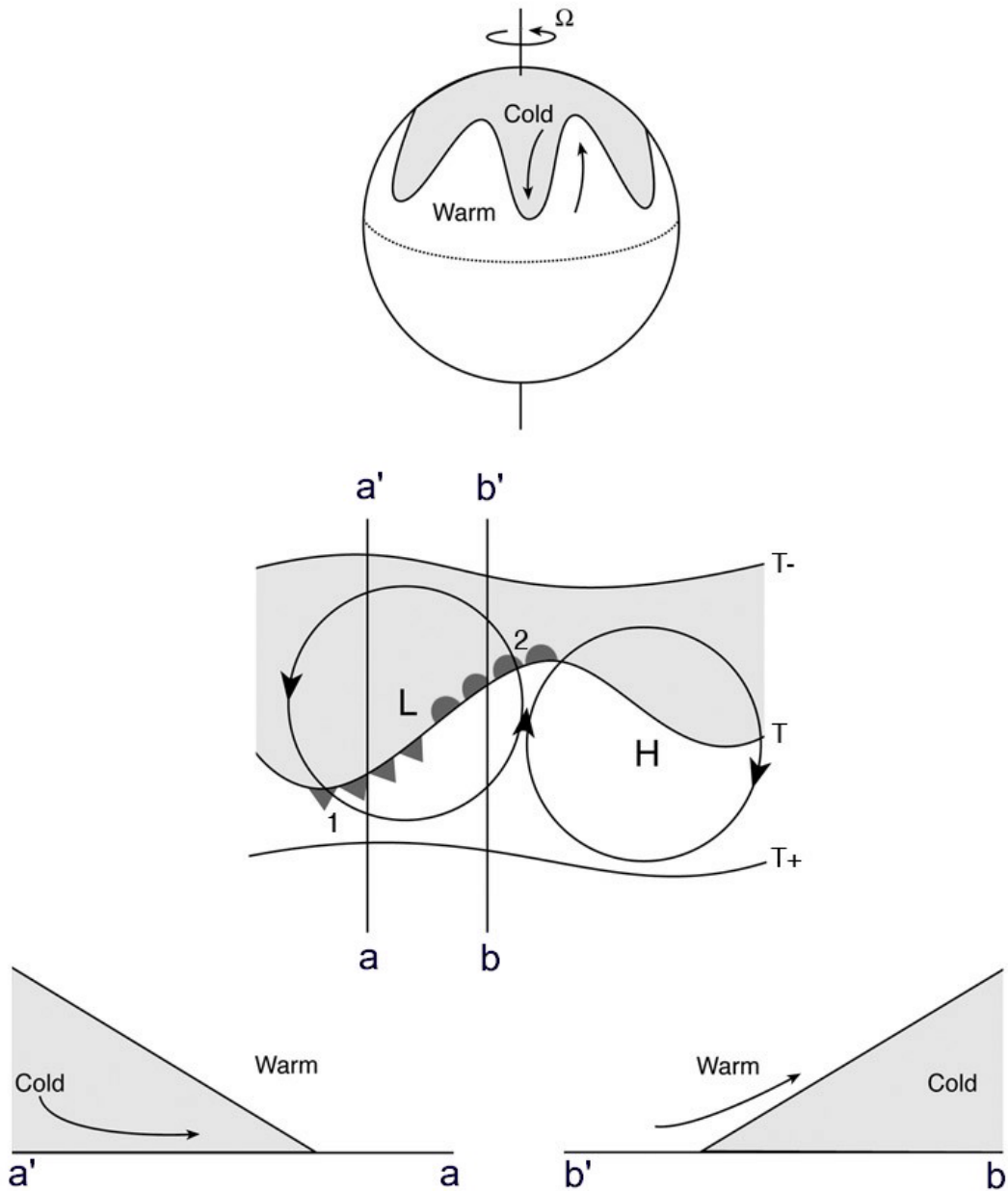


Figure 8.8: (top) In middle latitudes eddies transport warm air poleward and upward and cold air equatorward and downward. Thus, the eddies tend to “stir” the atmosphere laterally reducing the equator-to-pole temperature contrast. (middle) To the west of the ‘L’ cold air is carried in to the tropics. To the east, warm air is carried toward the pole. The resulting cold fronts (marked by triangles) and warm fronts (marked by semi-circles) are indicated. (bottom) Sections through the cold front, $a \rightarrow a'$, and the warm front, $b \rightarrow b'$, respectively.

from equator to pole, then we obtain unrealistically large winds. Angular momentum is not conserved because of the presence of zonal (or, in our tank experiment, azimuthal) pressure gradient associated with eddying motion (see Question 6 of Chapter 6).

Middle latitude weather systems The process of baroclinic instability studied in the above laboratory experiment is responsible for the ubiquitous waviness of the midlatitude flow in the atmosphere. As can be seen in the observations shown on Figs.5.22, 7.4 and 7.20, these waves often form closed eddies, especially near the surface, where they are familiar as the high and low pressure systems associated with day-to-day weather. In the process, they also affect the poleward heat transport required to balance global energy budget (see Fig.8.1). The manner in which this is achieved on the planetary scale is sketched in Fig.8.8: eddies “stir” the atmosphere carrying cold air equatorwards and warm air polewards, thereby reducing the equator-to-pole temperature contrast. To the west of the low (marked L) in Fig.8.8, cold air is carried into the tropics. To the east, warm air is carried toward the pole, but since poleward flowing air is ascending (remember the large-scale slope of the $\bar{\theta}$ surfaces shown in Fig.5.8) it tends to leave the surface. Thus we get a concentrated gradient of temperature near point 1 where the cold air ‘pushes into’ the warm air and a second, less marked, concentration where the warm air butts into cold at point 2. We can thus identify cold and warm fronts, respectively, as marked in the centre panel of Fig.8.8. Note that a triangle is used to represent the ‘sharp’ cold front and a semicircle to represent the ‘gentler’ warm front. In the bottom panel we present sections through cold fronts and warm fronts respectively.

Timescales and length scales We have demonstrated by laboratory experiment that a current in thermal wind balance can, and almost always does, become hydrodynamically unstable, spawning meanders and eddies. More detailed theoretical analysis⁶ shows that the lateral scale of the eddies

⁶Detailed analysis of the space-scales and growth rates of the instabilities that spontaneously arise on an initially zonal jet in thermal wind balance with a meridional temperature gradient show that:

1. the Eady growth rate of the disturbance $e^{\sigma t}$ is given by $\sigma = 0.31 \frac{U}{L_p} = 0.31 \frac{f}{N} \frac{d\bar{u}}{dz}$ using Eq.(7.23) and $U = \frac{d\bar{u}}{dz} H$ (see Gill, 1982). Inserting typical numbers for the troposphere — $N = 10^{-2} \text{ s}^{-1}$, $\frac{d\bar{u}}{dz} = 2 \times 10^{-3} \text{ s}^{-1}$, $f = 10^{-4} \text{ s}^{-1}$ — we find that

that form, L_{eddy} (as measured by, for example, the typical lateral scale of a low pressure systems in the surface analysis shown in Fig.7.25, or the swirls of dye seen in our tank experiment, Fig.8.7) is proportional to the Rossby radius of deformation discussed in Section 7.3.4:

$$L_{eddy} \sim L_\rho \quad (8.3)$$

where L_ρ is given by Eq.(7.23).

The time-scale of the disturbance is given by:

$$\mathcal{T}_{eddy} \sim \frac{L_\rho}{U} \quad (8.4)$$

where $U = \frac{d\bar{u}}{dz}H$ is the strength of the upper level flow, $\frac{d\bar{u}}{dz}$ is the thermal wind given by Eq.(7.17) and H is the vertical scale of the flow. Eq.(8.4) is readily interpretable as the time it takes a flow moving at speed U to travel a distance L_ρ and is proportional to the (inverse of) the ‘Eady growth rate’ after Eric Eady, a pioneer of the theory of baroclinic instability.

In our baroclinic instability experiment, we estimate a deformation radius of some 10 cm roughly in accord with the observed scale of the swirls in Fig.8.7 (to determine a scale, note that the diameter of the ice can in the figure is some 15 cm). Typical flow speeds observed by the tracking of paper dots floating at the surface of the fluid are about 1 cm s^{-1} . Thus Eq.(8.4) suggests a time-scale of $\mathcal{T}_{eddy} \sim 7.0 \text{ s}$ or, roughly, one rotation period. Consistent with Eq.(8.3), the eddy scale decreases with increased rotation rate.

Applying the above formulae to the middle troposphere where $f \sim 10^{-4} \text{ s}^{-1}$, $N \sim 10^{-2} \text{ s}^{-1}$ (see Section 4.4), $H \sim 7 \text{ km}$ (see Section 3.3) and $U \sim 10 \text{ m s}^{-1}$, we find that $L_\rho = \frac{NH}{f} \sim 700 \text{ km}$ and $\mathcal{T}_{eddy} \sim \frac{700 \text{ km}}{10 \text{ m s}^{-1}} \sim 1 \text{ d}$. These estimates are roughly in accord with the scales and growth rates of observed weather systems.

$\sigma \simeq 10^{-5} \text{ s}^{-1}$, an e -folding time-scale of 1 day.

2. the wavelength of the fastest growing disturbance is $4L_\rho$ where L_ρ is given by Eq.(7.23). This yields a wavelength of 2800 km if $L_\rho = 700 \text{ km}$. The circumference of the earth at 45° N is 21000 km and so about 7 synoptic waves can fit around the earth at any one time. This is roughly in accord with observations; see, for example, Fig.5.22.

We have not yet discussed the underlying baroclinic instability mechanism and its energy source. In order to do so we now consider the energetics of, and the release of potential energy from, a fluid.

8.3 Energetics of the thermal wind equation

The immediate source of kinetic energy for the eddy circulation observed in our baroclinic instability experiment and in the middle-latitude atmosphere, is the potential energy of the fluid. In the spirit of the energetic discussion of convection developed in Section 4.2.3, we now compute the potential energy available for conversion to motion. However, rather than, as there, considering the energy of isolated fluid parcels, here we focus on the potential energy of the whole fluid. It will become apparent that not all the potential energy of a fluid is available for conversion to kinetic energy. We need to identify that component of the potential energy—known as *available potential energy*—that can be released by a redistribution of mass of the system.

To keep things as simple as possible, we will first focus on an incompressible fluid, such as the water in our tank experiment. We will then go on to address the compressible atmosphere.

8.3.1 Potential energy for a fluid system

We assign to a fluid parcel of volume $dV = dx dy dz$ and density ρ , a potential energy of $gz \times (\text{parcel mass}) = gz\rho dV$. Then the potential energy of the entire fluid is

$$PE = g \int z\rho dV, \quad (8.5)$$

where the integral is over the whole system. Clearly, PE is a measure of the vertical distribution of mass.

Energy can be released and converted to kinetic energy only if some rearrangement of the fluid results in a lower total potential energy. Such rearrangement is subject to certain constraints, the most obvious of which is that the total mass

$$M = \int \rho dV, \quad (8.6)$$

cannot change. In fact, we may use Eq.(8.6) to rewrite Eq.(8.5) as

$$PE = gM \langle z \rangle \quad (8.7)$$

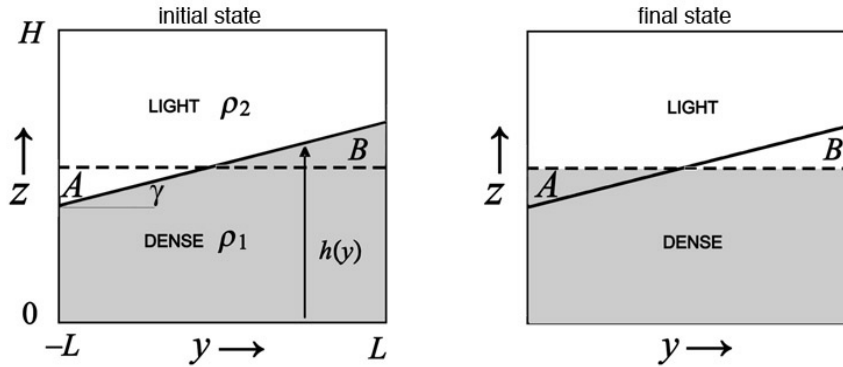


Figure 8.9: Reduction in the available potential energy of a two-layer fluid moving from an initial state in which the interface is tilted (left) to the final state in which the interface is horizontal (right). Dense fluid is shaded. The net effect of the rearrangement is to exchange heavy fluid downward and light fluid upward such that, in the wedge B , heavy fluid is replaced by light fluid, while the opposite occurs in the wedge A .

where

$$\langle z \rangle = \frac{\int z \rho \, dV}{\int \rho \, dV} = \frac{\int z \rho \, dV}{M} \quad (8.8)$$

is the mass-weighted mean *height* of the fluid. We can think of $\langle z \rangle$ as the ‘height of the center of mass’. It is evident from Eq.(8.7) that potential energy can be released only by lowering the center of mass of the fluid.

8.3.2 Available potential energy

Consider again the stratified incompressible fluid discussed in Section 4.2.2. Suppose, first, that $\partial\rho/\partial z < 0$ (stably stratified) and that there are no horizontal gradients of density, so ρ is a function of height *only*, as depicted in Fig.4.5. In Section 4.2.3 we considered the energetic implications of adiabatically switching the position of two parcels, initially at heights z_1 and z_2 , with densities ρ_1 and ρ_2 , respectively, with $z_2 > z_1$, and $\rho_2 < \rho_1$. Since ρ is conserved under the displacement (remember we are considering an incompressible fluid here), the final state has a parcel with density ρ_1 at z_2 , and one with ρ_2 at z_1 . Thus, density has increased at z_2 and decreased at z_1 . The center of mass has therefore been raised and so PE has been increased by

the rearrangement: none can be released into kinetic energy. This, of course, is one way of understanding why the stratification is stable. Even though such a fluid has nonzero potential energy (as defined by (8.7)), this energy is *unavailable* for conversion to kinetic energy: it cannot be reduced by any adiabatic rearrangement of fluid parcels. Therefore, the fluid has *available* potential energy only if it has nonzero horizontal gradients of density.⁷

Consider now the density distribution sketched in Fig.8.9(left); a two-layer fluid is shown with light fluid over heavy with the interface between the two sloping at angle γ . This can be considered to be a highly idealized representation of the radial density distribution in our tank experiment GFD Lab XI with heavier fluid (shaded) to the right (adjacent to the ice bucket) and light fluid to the left. Let us rearrange the fluid such that the interface becomes horizontal as shown. Now all fluid below the dashed horizontal line is dense, and all fluid above is light. The net effect of the rearrangement has been to exchange heavy fluid downward and light fluid upward such that, in the wedge B , heavy fluid has been replaced by light fluid, while the opposite has happened in the wedge A . (Such a rearrangement can be achieved in more than one way, as we shall see.) The center of mass has thus been lowered, and the final potential energy is therefore less than that in the initial state: potential energy has been released. Since no further energy can be released once the interface is horizontal, the difference in the potential energy between these two states defines the *available potential energy* (APE) of the initial state.

The important conclusions here are that available potential energy is associated with horizontal gradients of density and that release of that energy (and, by implication, conversion to kinetic energy of the motion) is effected by a reduction in those gradients.



⁷ Eric Eady (1918-1967). A brilliant theorist who was a forecaster in the early part of his career, Eady expounded the theory of baroclinic instability in a wonderfully lucid paper — Eady (1949) — which attempted to explain the scale, growth rate and structure of atmospheric weather systems.

The above discussion can be made quantitative as follows. Consider again Fig.8.9 in which the height of the interface between the two fluids is given by $h(y) = \frac{1}{2}H + \gamma y$ and, to keep things simple, we restrict the slope of the interface $\gamma < \frac{H}{2L}$ to ensure that it does not intersect the lower and upper boundaries at $z = 0$, $z = H$ respectively. Direct integration of Eq.(8.5) for the density distribution shown in Fig.8.9, shows that the potential energy per unit length in the x -direction is given by (as derived in the Appendix 13.1.2)

$$P = \int_0^H \int_{-L}^L g\rho z \, dy \, dz = H^2 L \rho_1 \left(g + \frac{g'}{4} \right) + \frac{1}{3} \rho_1 g' \gamma^2 L^3$$

where $g' = g \frac{(\rho_1 - \rho_2)}{\rho_1}$ is the reduced gravity of the system. P is at its absolute minimum, P_{\min} , when $\gamma = 0$, and given by the first term on the lhs of the above. When $\gamma = 0$, no rearrangement of fluid can lower the center of mass, since all dense fluid lies beneath all light fluid. When $\gamma \neq 0$, however, P exceeds P_{\min} , and the fluid has available potential energy in the amount

$$APE = P - P_{\min} = \frac{1}{3} \rho_1 g' \gamma^2 L^3. \quad (8.9)$$

Note that APE is independent of depth H because all the APE is associated with the interfacial slope; only fluid motion in the vicinity of the interface changes potential energy, as is obvious by inspection of Fig.8.9.

It is interesting to compare the APE associated with the tilted interface in Fig.8.9 with the kinetic energy associated with the thermal wind current which is in balance with it. Making use of Margules formula, Eq.(7.21), the geostrophic flow of the upper layer is given by $u_2 = g' \frac{\gamma}{2\Omega}$ if the lower layer is at rest. Thus the kinetic energy of the flow per unit length is, on evaluation:

$$KE = \int_h^H \int_{-L}^L \frac{1}{2} \rho_2 u_2^2 \, dy \, dz = \frac{1}{2} \rho_2 \frac{g'^2 \gamma^2}{(2\Omega)^2} HL \quad (8.10)$$

The ratio of APE to KE is thus:

$$\frac{APE}{KE} = \frac{2}{3} \left(\frac{L}{L_\rho} \right)^2 \quad (8.11)$$

where we have set $\frac{\rho_1}{\rho_2} \rightarrow 1$ and used Eq.(7.23) to express the result in terms of the deformation radius L_ρ .

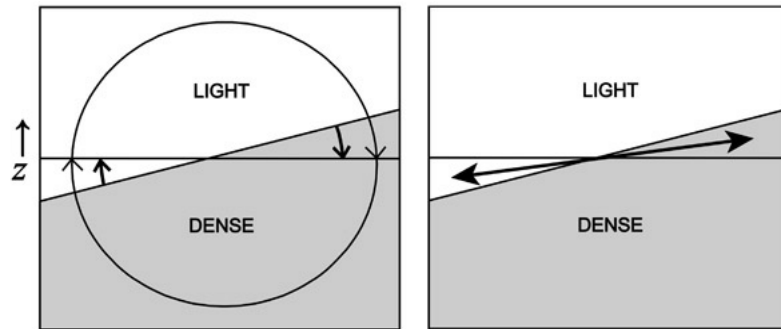


Figure 8.10: Release of available potential energy in a two-component fluid. (left) Non-rotating (or very slowly rotating) case: azimuthally uniform overturning. (right) Rapidly rotating case: sloping exchange in the wedge of instability by baroclinic eddies.

Eq.(8.11) is a rather general result for balanced flows — the ratio of APE to KE is proportional to the square of the ratio of L , the lateral scale over which the flow changes, to the deformation radius L_ρ . Typically, on the large-scale, L is considerably larger than L_ρ and so the potential energy stored in the sloping density surfaces greatly exceeds the kinetic energy associated with the thermal wind current in balance with it. For example, T varies on horizontal scales of $L \sim 5000$ km in Fig.5.7. In Section 8.2.2 we estimated that $L_\rho \sim 700$ km: thus $(L/L_\rho)^2 \simeq 50$. This has important implications for atmospheric and (as we shall see in Chapter 10) oceanic circulation⁸.

8.3.3 Release of Available Potential Energy in baroclinic instability

In a non-rotating fluid, the release of APE is straightforward and intuitive. If, at some instant in time, the interface of our two-component fluid were tilted as shown in Fig.8.10(left), we would expect the interface to collapse in the manner depicted by the heavy arrows in the figure. In reality, the interface would overshoot the horizontal position, and the fluid would slosh

⁸In fact in the ocean $\left(\frac{L}{L_\rho}\right)^2 \simeq 400$ telling us that the available potential energy stored in the main thermocline exceeds the kinetic energy associated with ocean currents by a factor of 400. (See Section 10.5.)

around until friction brought about a motionless steady state with the interface horizontal. The *APE* released by this process would first have been converted to kinetic energy of the motion, and ultimately lost to frictional dissipation. In this case, there would be no circulation in the long term, but if external factors such as heating at the left of Fig.8.10(left) and cooling at the right were to sustain the tilt in the interface, there would be a steady circulation (shown by the light arrows in the figure) in which the interface-flattening effects of the circulation balance the heating and cooling.

In a rotating fluid, things are not so obvious. There is no necessity for a circulation of the type shown in Fig.8.10(left) to develop since, as we saw in Section 7.3.5, an equilibrium state can be achieved in which forces associated with the horizontal density gradient are in thermal wind balance with a vertical shear of the horizontal flow. In fact, rotation actively suppresses such circulations. We have seen that if Ω is sufficiently small, as in the Hadley circulation experiment GFD Lab VIII (section 8.2.1), such a circulation is indeed established. At high rotation rates, however, a Hadley regime is not observed; nevertheless, *APE* can still be released, albeit by a very different mechanism. As we discussed in Section 8.2.2, the zonal state we have described is *unstable to baroclinic instability*. Through this instability, azimuthally asymmetric motions are generated, within which fluid parcels are exchanged along sloping surfaces as they oscillate from side to side, as sketched in Fig.8.8. The azimuthal current is therefore not purely zonal, but wavy, as observed in the laboratory experiment shown in Fig.8.7. The only way light fluid can be moved upward in exchange for downward motion of heavy fluid is for the exchange to take place at an angle that is steeper than the horizontal, but less steep than the density surfaces, *i.e.*, within the so-called *wedge of instability*, as shown in Fig.8.10(right). Thus, *APE* is reduced, not by overturning in the radial plane, but by fluid parcels oscillating back and forth within this wedge: light (warm) fluid moves upwards and radially inwards at one azimuth while, simultaneously, heavy (cold) fluid moves downwards and outwards at another as sketched in Fig.8.8. This is

the mechanism at work in GFD Lab XI.⁹

8.3.4 Energetics in a compressible atmosphere

So far we have discussed energetics in the context of an incompressible fluid such as water. However, it is not immediately clear how we can apply concepts such as available potential energy to a compressible fluid such as the atmosphere. Parcels of incompressible fluid can do no work on their surroundings and T is conserved in adiabatic rearrangement of the fluid: potential energy is all one needs to consider. However, air parcels expand and contract during the redistribution of mass, doing work on their surroundings and changing their T and hence internal energy. Thus we must also consider changes in *internal energy*. It turns out that, for an atmosphere in hydrostatic balance and with a flat lower boundary, it is very easy to extend the definition Eq.(8.5) to include the internal energy. The internal energy (IE) of the entire atmosphere (assuming it to be a perfect gas) is, if we neglect surface topography (see Appendix 13.1.3)

$$IE = c_v \int \rho T dV = \frac{c_v}{R} g \int z \rho dV . \quad (8.12)$$

Note the similarity with Eq.(8.5): in fact, for a diatomic gas like the atmosphere, $c_v/R = (1 - \kappa)/\kappa = 5/2$, so its internal energy (neglecting topographic effects) is 2.5 times greater than its potential energy. The sum of internal and potential energy is conventionally (if somewhat loosely) referred to as *total potential energy*, and given by



⁹ Jule Gregory Charney (1917-1981), American meteorologist and MIT Professor. He made wide-ranging contributions to the modern mathematical theory of atmospheric and oceanic dynamics, including the theory of large-scale waves, and of baroclinic instability. He was also one of the pioneers of numerical weather prediction, producing the first computer forecast in 1950.

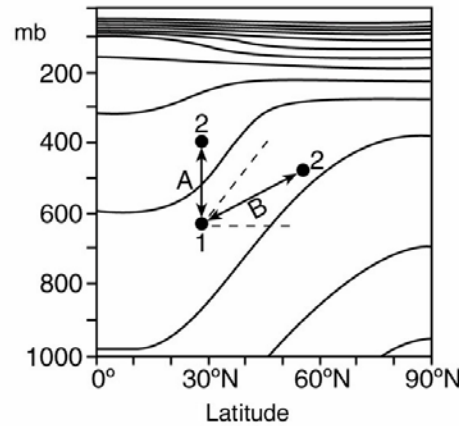


Figure 8.11: Air parcels ‘1’ and ‘2’ are exchanged along paths marked A and B conserving potential temperature θ . The continuous lines are observed θ surfaces — see Fig. 5.8. The tilted dotted line is parallel to the local θ .

$$TPE = PE + IE = \frac{g}{\kappa} \int z \rho dV = \frac{g}{\kappa} M \langle z \rangle \quad (8.13)$$

where, as before, $\langle z \rangle$ is defined by Eq.(8.8) and M by Eq.(8.6).

We can apply the ideas discussed in the previous section to a compressible fluids if, as discussed in Chapter 4, we think in terms of the distribution of potential temperature, rather than density, since the former is conserved under adiabatic displacement.

Consider Fig.8.11 in which the distribution of θ in the atmosphere, θ increasing upward and equatorward as in Fig.5.8, is schematically shown. Again, we suppose that two air parcels are exchanged adiabatically. Suppose first that we exchange parcel 1, with $\theta = \theta_1$, with a second parcel with $\theta = \theta_2 > \theta_1$, vertically along path A. It is clear that the final potential energy will be greater than the initial value because the parcel moving upward is colder than the parcel it replaces. This is just the problem considered in our study of stability conditions for dry convection in Section 4.3. If parcels are exchanged along a horizontal path or along a path in a surface of constant θ (dotted lines in the figure), there will be no change in potential energy. But consider exchanging parcels along path B in Fig.8.11, which has a slope *between* that of the θ surface and the horizontal. The parcel moving upwards

is now warmer than the parcel moving downwards and so potential energy has been reduced by the parcel rearrangement. In other words the center of gravity of the fluid is lowered. In the process, a lateral transport of heat is achieved from cold to warm. It is this release of APE that powers the eddying motion. As discussed in Section 8.3.3, fluid parcels are exchanged in this ‘wedge of instability’ as they oscillate from side to side, as sketched in Fig.8.8.

8.4 Large-scale atmospheric heat and momentum budget

8.4.1 Heat transport

We have seen two basic facts about the atmospheric energy budget:

1. There must be a *conversion* of energy into kinetic energy, from the available potential energy gained from solar heating, which requires that motions develop which transport heat upward (thereby tending to lower the atmospheric center of mass).
2. Accompanying this upward transport, there must be a *poleward transport* of heat from low latitudes; this transport cools the tropics and heats the polar regions, thus balancing the observed radiative budget.

It is fairly straightforward to estimate the rate of poleward heat transport by atmospheric motions. Consider the northward flow at latitude φ across an elemental area dA , of height dz and longitudinal width $d\lambda$, so $dA = a \cos \varphi d\lambda dz$. The rate at which mass is flowing northward across dA is $\rho v dA$, and the associated flux of energy is $\rho v E dA$, where

$$E = c_p T + gz + Lq + \frac{1}{2} \mathbf{u} \cdot \mathbf{u} \quad (8.14)$$

is the moist static energy, Eq.(4.27) (made up of the “dry static energy” $c_p T + gz$, and the latent heat content Lq) and the kinetic energy density $\frac{1}{2} \mathbf{u} \cdot \mathbf{u}$. If we now integrate across the entire atmospheric surface at that

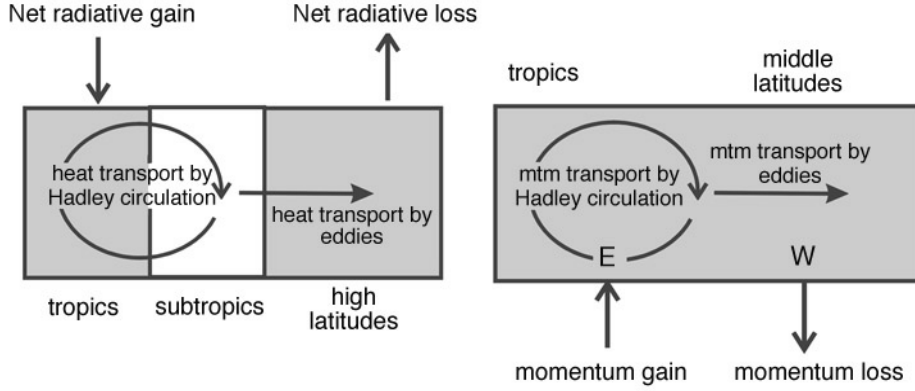


Figure 8.12: Schematic of the transport of (left) energy and (right) momentum by the atmospheric general circulation. Transport occurs through the agency of the Hadley circulation in the tropics, and baroclinic eddies in middle latitudes — see also Fig.8.1.

latitude, the net energy flux is

$$\begin{aligned}
 \overline{\mathcal{H}}_{atmos}^{\lambda} &= \iint \rho v E \, dA \\
 &= a \cos \varphi \int_0^{2\pi} \int_0^{\infty} \rho v E \, dz \, d\lambda \\
 &= \frac{a}{g} \cos \varphi \int_0^{2\pi} \int_0^{p_s} v E \, dp \, d\lambda , \quad (8.15)
 \end{aligned}$$

(using hydrostatic balance to replace ρdz by $-dp/\rho$) where p_s is surface pressure. It turns out that the kinetic energy component of the net transport is negligible (typically less than 1% of the total), so we only need to consider the first three terms in Eq.(8.14).

Let us first consider energy transport in the tropics by the Hadley circulation which (in the annual mean) has equatorward flow in the lower troposphere and poleward flow in the upper troposphere. We may write

$$\overline{\mathcal{H}}_{tropics}^{\lambda} = \frac{2\pi a}{g} \cos \varphi \int_0^{p_s} v (c_p T + gz + Lq) \, dp . \quad (8.16)$$

where we have assumed that the tropical atmosphere is independent of longitude λ .

Since temperature decreases with altitude, the heat carried poleward by the upper tropospheric flow is less than that carried equatorward at lower altitudes. Therefore the net heat transport — the first term in Eq.(8.16) — is equatorward: the Hadley circulation carries heat toward the hot equator from the cooler subtropics! This does not seem very sensible. However, now let us add in the second term in Eq.(8.16), the potential energy density gz , to obtain the flux of dry static energy $v(c_p T + gz)$. Note that the vertical gradient of dry static energy is $\partial(c_p T + gz)/\partial z = c_p \partial T/\partial z + g$. For an atmosphere (like ours) that is generally stable to dry convection, $\partial T/\partial z + g/c_p > 0$ (as discussed in Section 4.3.1) and so the dry static energy increases with height. Therefore the poleward flow at high altitude carries more dry static energy poleward than the low-level flow takes equatorward, and the net transport is poleward, as we might expect.

To compute the total energy flux we must include all the terms in Eq.(8.16). The latent heat flux contribution is equatorward, since (see Fig.5.15) q decreases rapidly with height, and so the equatorward flowing air in the lower troposphere carries more moisture than the poleward moving branch aloft. In fact, this term almost cancels the dry static energy flux. This is because the gross vertical gradient of moist static energy $c_p T + gz + Lq$ — a first integral of Eq.(4.26) under hydrostatic motion — is weak in the tropics. This is just another way of saying that the tropical atmosphere is almost neutral to moist convection, a state that moist convection itself helps to bring about. This is clearly seen in the profiles of moist potential temperature shown in Fig.5.9 of Chapter 5. Thus the equatorward and poleward branches of the circulation carry almost the same amount in each direction. In the net, then, the annually averaged energy flux by the Hadley cell is poleward, but weakly so. In fact, as can be seen in Fig.8.13, the heat transport by the ocean exceeds that of the atmosphere in the tropics up to 15° or so, particularly in the northern hemisphere.

The relative contributions of the various components of the energy flux are different in the extra-tropics, where the mean circulation is weak and essentially all the transport is effected by midlatitude eddies. In these motions, the poleward and equatorward flows occur at almost the same altitude, and so the strong vertical gradients of gz and Lq are not so important. While these components of the energy flux are not entirely negligible (and must be accounted for in any detailed calculation), they are relatively small and so we can use the heat flux alone to obtain a reasonable estimate of the net flux.

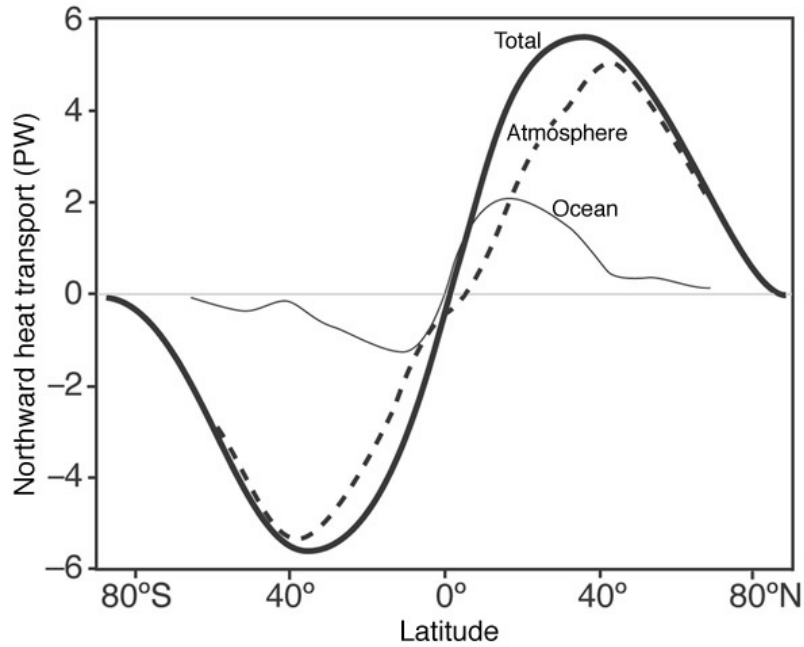


Figure 8.13: The Ocean (thin) and Atmospheric (dotted) contributions to the total northwards heat flux (thick) based on the NCEP reanalysis (in $\text{PW} = 10^{15}\text{W}$) by (i) estimating the net surface heat flux over the ocean (ii) the associated oceanic contribution, correcting for heat storage associated with global warming and constraining the ocean heat transport to be -0.1 PW at 68°S (iii) deducing the atmospheric contribution as a residual. The total meridional heat flux, as in Fig.5.6, is also plotted (thick). From Trenberth and Caron (2001).

So in middle latitudes we can represent Eq.(8.15) by

$$\overline{\mathcal{H}}_{mid-lat}^{\lambda} \sim 2\pi \frac{ac_p}{g} \cos \varphi p_s [v][T]$$

where $[v]$ is a typical northward wind velocity (dominated by the eddy component in middle latitudes) and $[T]$ is the typical magnitude of the temperature *fluctuations* in the presence of the eddies—the temperature difference between equatorward and poleward flowing air. Given $a = 6371$ km, $c_p = 1005$ J kg⁻¹ K⁻¹, $g = 9.81$ m s⁻², $p_s \simeq 10^5$ Pa, then if we take typical values of $[v] \simeq 10$ m s⁻¹ and $[T] \simeq 3$ K at a latitude of 45°, we estimate $\overline{\mathcal{H}}_{mid-lat}^{\lambda} \sim 8$ PW. As discussed earlier in Section 5.1.3 and in more detail below, this is of the same order as implied by the radiative imbalance.

In cartoon form, our picture of the low- and high-latitude energy balance is therefore as shown in Fig.8.12(left). In the tropics energy is transported poleward by the Hadley circulation; in higher latitudes eddies are the principal agency of heat transport.

The results of more complete calculations, making use of top of the atmosphere radiation measurements and analyzed atmospheric fields, of heat fluxes in the atmosphere and ocean are shown in Fig.8.13. The bulk of the required transport is carried by the atmosphere in middle and high latitudes, but the ocean makes up a considerable fraction, particularly in the tropics where (as we have seen) atmospheric energy transport is weak. The role of the ocean in meridional heat transport, and the partition of heat transport between the atmosphere and ocean, are discussed in some detail in Section 11.5.2.

8.4.2 Momentum transport

In addition to transporting heat, the general circulation also transports angular momentum. In the Hadley circulation, as we have seen, the upper, poleward-flowing, branch is associated with strong westerly winds: thus, westerly momentum is carried poleward. The lower branch, on the other hand, is associated with easterlies that are weakened by surface friction; the equatorward flow carries weak easterly momentum equatorward. The net effect is a poleward transport of westerly angular momentum. Midlatitude eddies also transport angular momentum (albeit for less obvious and, in fact, quite subtle reasons, as sketched in Fig.8.14), again mostly transporting eastward angular momentum poleward. This has the effect of modifying the

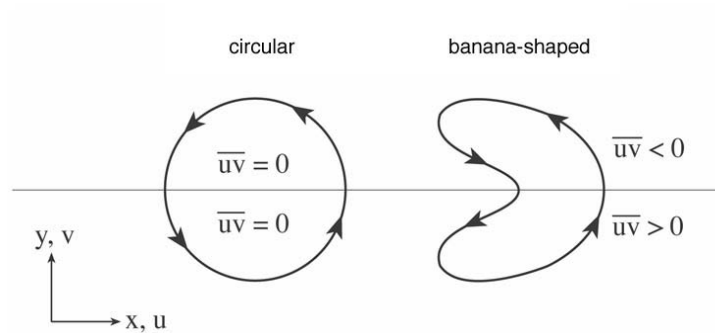


Figure 8.14: Circular eddies on the left are unable to affect a meridional transfer of momentum. The eddies on the right, however, by virtue of their ‘banana shape’, transfer westerly momentum northwards south of, and southwards north of, the mid-line. Weather systems transport westerly momentum from the tropics ($\overline{uv} > 0$) towards higher latitudes, as required in Fig.8.12(right), by ‘trailing’ their troughs down in to the tropics (see, e.g., the H_2O distribution shown in Fig.3), as in the southern half of the ‘banana-shaped’ eddy sketched on the right.

surface winds from that sketched schematically in Fig.8.5, by shifting the low latitude westerlies into middle latitudes.

The atmospheric angular momentum budget may therefore be depicted as in Fig.8.12(right). Because there is a net export of momentum out of low latitudes, there must be a supply of momentum into this region; the only place it can come from is the surface, through friction acting on the low level winds. In order for the friction to supply angular momentum to the atmosphere (and yet act as a brake on the low level winds) the low level winds in the tropics must be easterly, consistent with that deduced for the Hadley circulation here. The balancing loss of westerly momentum from the atmosphere — which must be associated with drag on the near-surface westerlies — is located in middle latitudes and balances the supply of westerly momentum via eddy transport.

8.5 Latitudinal variations of climate

Putting everything together, we can depict the atmospheric wind systems in the upper and lower troposphere schematically as in Fig.8.15.

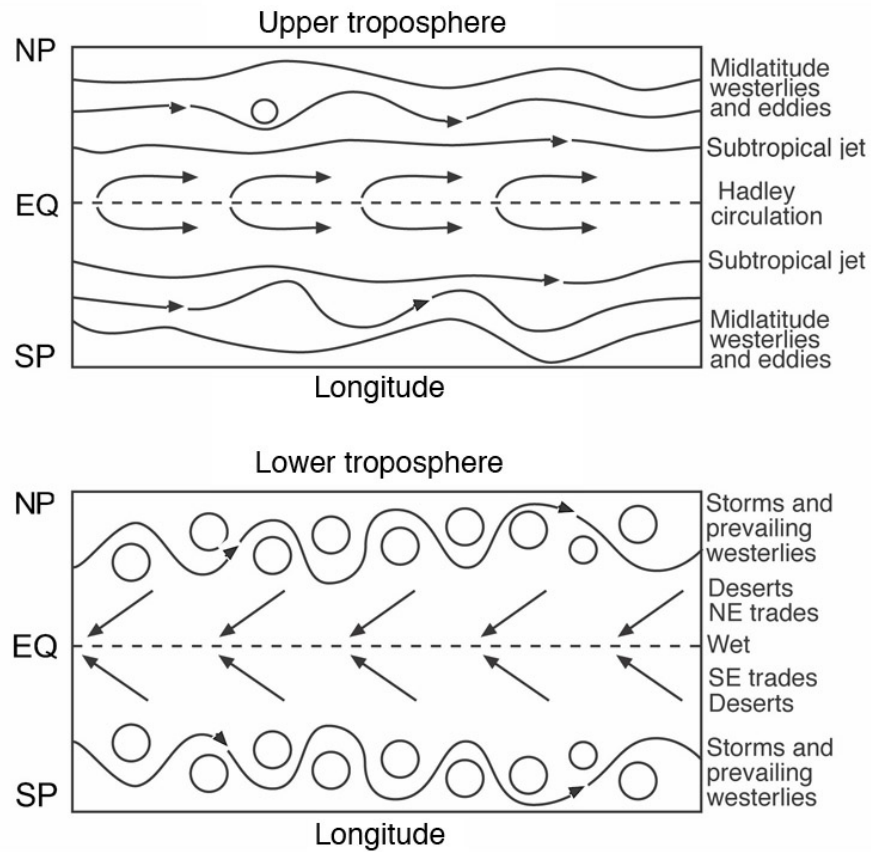


Figure 8.15: Schematic of the global distributions of atmospheric winds in the upper (top) and lower (bottom) troposphere together with the primary latitudinal climate zones.

As we have remarked at various points along the way in this chapter, the structure of the circulation dictates more than just the pattern of winds. In the near-equatorial regions, the convergence of the trade winds is associated with frequent and intense rainfall, as is characteristic of the deep tropics; it is here, for example, that the world's great tropical rainforests are located. Around the subtropics ($20^\circ - 30^\circ$ latitude), in the warm, dry, descending branch of the Hadley circulation, the climate is hot and dry: this is the subtropical desert belt. Poleward of about 30° , where baroclinic eddies dominate the meteorology, local winds vary from day to day, though they are predominantly westerly, and the weather is at the mercy of the passing eddies: usually calm and fine in anticyclonic high pressure systems, and frequently wet and stormy in cyclonic, low pressure systems.

At least from a "big picture" viewpoint, we have thus been able to deduce the observed pattern of atmospheric winds, and the division of the world into major climate zones, through straightforward consideration of the properties of a dynamic atmosphere on a longitudinally uniform rotating planet subject to longitudinally independent differential heating. We cannot proceed much further without taking account of seasonal variations, and of longitudinal asymmetry of the Earth, which we do not have the space to develop here. However, we will briefly note some of the major differences between our simple picture and observed circulation.

During the course of a year, the pattern of solar forcing migrates, north in northern summer, south in southern summer, and this has a significant impact on the atmospheric response. Our picture of the "typical" Hadley circulation (Fig.8.5) inevitably shows symmetry about the equator. In reality, the whole circulation tends to shift seasonally such that the upwelling branch and associated rainfall are found on the summer side of the equator (see Fig.5.21). The degree to which this happens is strongly controlled by local geography: seasonal variations over the oceans, whose temperature varies relatively little through the year, are weak, while they are much stronger over land. The migration of the main area of rainfall is most dramatic in the region of the Indian Ocean, where intense rain moves onto the Asian continent during the summer monsoon.

While prevailing westerlies and migrating storms characterize most of the extratropical region throughout the year, there are seasonal variations (generally with more storms in winter, when the temperature gradients are greater, than in summer) and strong longitudinal variations, mostly associated with the distribution of land and sea. Longitudinal variations in climate can be

dramatic: consider the contrast across the Atlantic Ocean, where the January mean temperature at Goose Bay, Newfoundland (at about 53°N) is about 30°C colder than that at Galway, at almost the same latitude on the west coast of Ireland. We cannot explain this with our longitudinally symmetric model of the world, but the explanation is nevertheless straightforward. Prevailing winds bring cold continental air to the coast of Newfoundland, but mild oceanic air to the west coast of Ireland. The North Atlantic Ocean is much warmer than the continents at the same latitude in winter, partly because of the large heat capacity of the ocean, and partly because of heat transport by the ocean circulation. The ocean circulation and its role in climate is the subject of the following Chapters.

8.6 Further reading

An interesting historical account of evolving perspectives on the general circulation of the atmosphere is given in Lorenz (1967). Chapter 6 of Hartmann (1994) presents a thorough discussion of the energy and angular budgets of the general circulation; a more advanced treatment can be found in Chapter 10 of Holton (2004).

8.7 Problems

1. Consider a zonally symmetric circulation (*i.e.*, one with no longitudinal variations) in the atmosphere. In the inviscid upper troposphere, one expects such a flow to conserve absolute angular momentum, *i.e.*, $DA/Dt = 0$, where $A = \Omega a^2 \cos^2 \varphi + ua \cos \varphi$ is the absolute angular momentum per unit mass — see Eq.(8.1) — where Ω is the Earth rotation rate, u the eastward wind component, a the Earth's radius, and φ latitude.
 - (a) Show, for inviscid zonally symmetric flow, that the relation $DA/Dt = 0$ is consistent with the zonal component of the equation of motion (using our standard notation, with \mathcal{F}_x the x -component of the friction force per unit mass)

$$\frac{Du}{Dt} - fv = -\frac{1}{\rho} \frac{\partial p}{\partial x} + \mathcal{F}_x ,$$

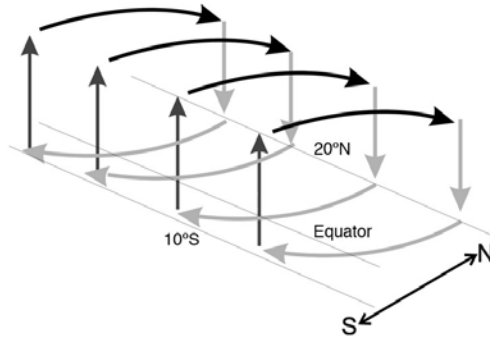


Figure 8.16: A schematic diagram of the Hadley circulation rising at 10°S , crossing the equator and sinking at 20°N .

in (x, y, z) coordinates, where $y = a\varphi$ (see Fig.6.19).

- (b) Use angular momentum conservation to describe how the existence of the Hadley circulation explains the existence of both the subtropical jet in the upper troposphere and the near-surface Trade Winds.
 - (c) If the Hadley circulation is symmetric about the equator, and its edge is at 20° latitude, determine the strength of the subtropical jet.
2. Consider the tropical Hadley circulation in northern winter, as shown in Fig.8.16. The circulation rises at 10°S , moves northward across the equator in the upper troposphere, and sinks at 20°N . Assuming that the circulation, outside the near-surface boundary layer, is zonally symmetric (independent of x) and inviscid (and thus conserves absolute angular momentum about the Earth's rotation axis), and that it leaves the boundary layer at 10°S with zonal velocity $u = 0$, calculate the zonal wind in the upper troposphere at (a) the equator, (b) at 10°N , and (c) at 20°N .
 3. Consider what would happen if a force toward the pole were applied to the ring of air considered in Q.1 if it conserved its absolute angular momentum, A . Calculate the implied relationship between a small displacement $\delta\varphi$ and the change in the speed of the ring δu . How many

kilometers northwards does the ring have to be displaced in order to change its relative velocity 10 m s^{-1} ? How does your answer depend on the equilibrium latitude? Comment on your result.

4. An open dish of water is rotating about a vertical axis at 1 revolution per minute. Given that the water is 1°C warmer at the edges than at the center at all depths, estimate, under stated assumptions and using the data below, typical azimuthal flow speeds at the free surface relative to the dish. Comment on, and give a physical explanation for, the sign of the flow.

How much does the free surface deviate from its solid body rotation form?

Briefly discuss ways in which this rotating dish experiment is a useful analogue of the general circulation of the Earth's atmosphere.

Assume the equation of state given by Eq.(4.4) with $\rho_{ref} = 1000 \text{ kg m}^{-3}$, $\alpha = 2 \times 10^{-4} \text{ K}^{-1}$ and $T_{ref} = 15^\circ\text{C}$, the mean temperature of the water in the dish. The dish has a radius of 10 cm and is filled to a depth of 5 cm.

5. Consider the incompressible, baroclinic fluid ($\rho = \rho(T)$) sketched in Fig.8.17 in which temperature surfaces slope upward toward the pole at an angle s_1 . Describe the attendant zonal wind field assuming it is in thermal wind balance.

By computing the potential energy before and after interchange of two rings of fluid (coincident with latitude circles y at height z) along a surface of slope s , show that the change in potential energy $\Delta PE = PE_{final} - PE_{initial}$ is given by

$$\Delta PE = \rho_{ref} N^2 (y_2 - y_1)^2 s (s - s_1),$$

where $N^2 = -\frac{g}{\rho_{ref}} \frac{\partial \rho}{\partial z}$ is the buoyancy frequency (see Section 4.4), ρ_{ref} is the reference density of the fluid and y_1, y_2 are the latitudes of the interchanged rings. You will find it useful to review Section 4.2.3.

Hence show that for a given meridional exchange distance $(y_2 - y_1)$:

- (a) energy is released if $s < s_1$

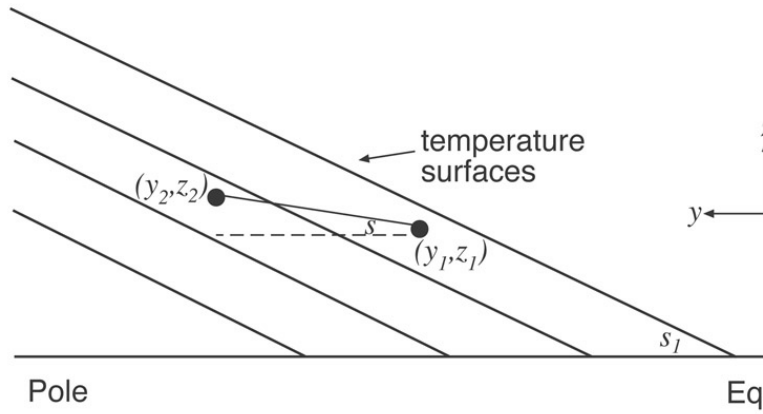


Figure 8.17: Schematic for energetic analysis of the thermal wind considered in Q.5. Temperature surfaces have slope s_1 : parcels of fluid are exchanged along surfaces which have a slope s .

- (b) the energy released is a maximum when the exchange occurs along surfaces inclined at *half* the slope of the temperature surfaces.

This is the ‘wedge of instability’ discussed in Section 8.3.3 and illustrated in Fig.8.10.

6. Discuss qualitatively, but from basic principles, why most of the Earth’s desert regions are found at latitudes of $\pm (20^\circ - 30^\circ)$.
7. Given that the heat content of an elementary mass dm of air at temperature T is $c_p T dm$ (where c_p is the specific heat of air at constant pressure), and that its northward velocity is v :
- (a) show that the northward flux of heat crossing unit area (in the $x - z$ plane) per unit time is $\rho c_p v T$;
- (b) hence, using the hydrostatic relationship, show that the net northward heat flux \mathcal{H} in the atmosphere, at any given latitude, can be written

$$\mathcal{H} = c_p \int_{x_1}^{x_2} \int_0^\infty \rho v T dx dz = \frac{c_p}{g} \int_{x_1}^{x_2} \int_0^{p_s} v T dx dp ,$$

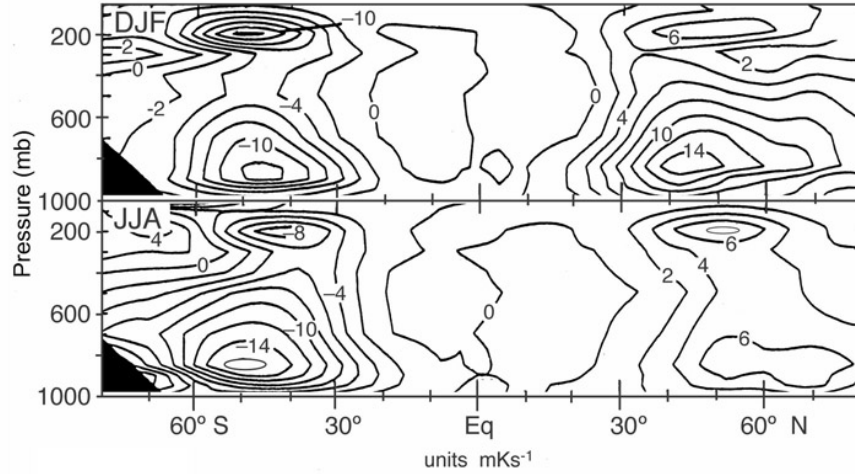


Figure 8.18: The contribution by eddies (K m s^{-1}) to the meridional flux \overline{vT} (Eq.8.17), plotted as a function of latitude and pressure for (top) DJF and (bottom) JJA.

where the first integral (in x) is completely around a latitude circle and p_s is surface pressure.

- (c) Fig.8.18 shows the contribution of eddies to the atmospheric heat flux.

What is actually shown is the contribution of eddies to the quantity \overline{vT} , which in the above notation is

$$\overline{vT} = \frac{1}{x_2 - x_1} \int_{x_1}^{x_2} vT \, dx \quad (8.17)$$

(i.e., the zonal average of vT), where $x_2 - x_1 = 2\pi a \cos \varphi$, where a is the Earth radius and φ latitude. Use the figure to *estimate* the net northward heat flux by eddies across 45°N . Compare this with the requirement (from the Earth's radiation budget and Fig.8.13) that the net (atmosphere and ocean) heat transport must be about $5 \times 10^{15}\text{W}$.